

See discussions, stats, and author profiles for this publication at: <https://www.researchgate.net/publication/51129030>

# Facile Synthesis of Degradable and Electrically Conductive Polysaccharide Hydrogels

ARTICLE in BIOMACROMOLECULES · MAY 2011

Impact Factor: 5.75 · DOI: 10.1021/bm200389t · Source: PubMed

CITATIONS

52

READS

54

## 3 AUTHORS:



**Baolin Guo**

Xi'an Jiaotong University

41 PUBLICATIONS 652 CITATIONS

[SEE PROFILE](#)



**Anna Finne-Wistrand**

KTH Royal Institute of Technology

86 PUBLICATIONS 1,392 CITATIONS

[SEE PROFILE](#)



**Ann-Christine Albertsson**

KTH Royal Institute of Technology

419 PUBLICATIONS 11,374 CITATIONS

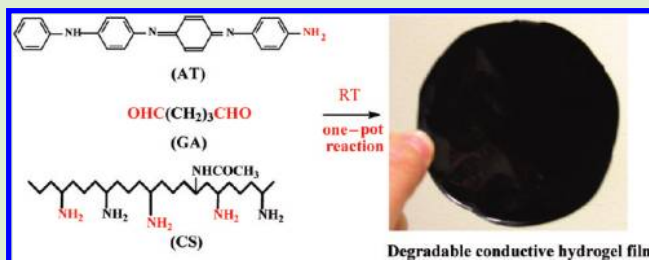
[SEE PROFILE](#)

# Facile Synthesis of Degradable and Electrically Conductive Polysaccharide Hydrogels

Baolin Guo, Anna Finne-Wistrand, and Ann-Christine Albertsson\*

Department of Fibre and Polymer Technology, School of Chemical Science and Engineering, Royal Institute of Technology, SE-100 44, Stockholm, Sweden

**ABSTRACT:** Degradable and electrically conductive polysaccharide hydrogels (DECPHs) have been synthesized by functionalizing polysaccharide with conductive aniline oligomers. DECPHs based on chitosan (CS), aniline tetramer (AT), and glutaraldehyde were obtained by a facile one-pot reaction by using the amine group of CS and AT under mild conditions, which avoids the multistep reactions and tedious purification involved in the synthesis of degradable conductive hydrogels in our previous work. Interestingly, these one-pot hydrogels possess good film-forming properties, electrical conductivity, and a pH-sensitive swelling behavior. The chemical structure and morphology before and after swelling of the hydrogels were verified by FT-IR, NMR, and SEM. The conductivity of the hydrogels was tuned by adjusting the content of AT. The swelling ratio of the hydrogels was altered by the content of tetraaniline and cross-linker. The hydrogels underwent slow degradation in a buffer solution. The hydrogels obtained by this facile approach provide new possibilities in biomedical applications, for example, biodegradable conductive hydrogels, films, and scaffolds for cardiovascular tissue engineering and controlled drug delivery.



## INTRODUCTION

Hydrogels from natural polymers, especially polysaccharides, have attracted increasing attention recently because of their excellent biocompatibility, biodegradation, nontoxicity, and abundant and ready availability from renewable sources.<sup>1–4</sup> Polysaccharides contain a large amount of hydroxyl groups in their structure, and this makes chemical modification very easy.<sup>5–8</sup> Among all polysaccharides, chitosan (CS) is the only natural cationic polymer. CS has good biodegradability, biocompatibility, immunological, antibacterial, and wound-healing activity and good mechanical and film-forming properties. CS has been widely used for controlled drug delivery,<sup>9,10</sup> and it is a good candidate for gene delivery, cell culture, and tissue engineering.<sup>11,12</sup> It has a large number of amino groups and hydroxyl groups along the main chains, and it can dissolve in aqueous acid solution, which offers the possibility for easy functionalization.<sup>12–15</sup> We have synthesized pH-sensitive hydrogels by grafting lactic acid and glycolic acid onto the CS. The thermal degradation kinetics, swelling behavior, and state of water of the hydrogels were investigated, and these hydrogels have a great potential in biomedical application.<sup>15–17</sup> CS is easily cross-linked by glutaraldehyde (GA) to generate CS hydrogels, and these hydrogels are pH-sensitive and are widely used in drug delivery systems, artificial muscles, and tissue engineering.<sup>18–20</sup> For drug delivery to the stomach, a pH 2.1 buffer solution is commonly used to simulate the gastric fluid,<sup>21,22</sup> which is pertinent because it is one of the potential applications of the hydrogels discussed in this work.

Recent research shows that electrical stimulation can affect a range of cellular activities.<sup>23,24</sup> Conducting polymers, such as

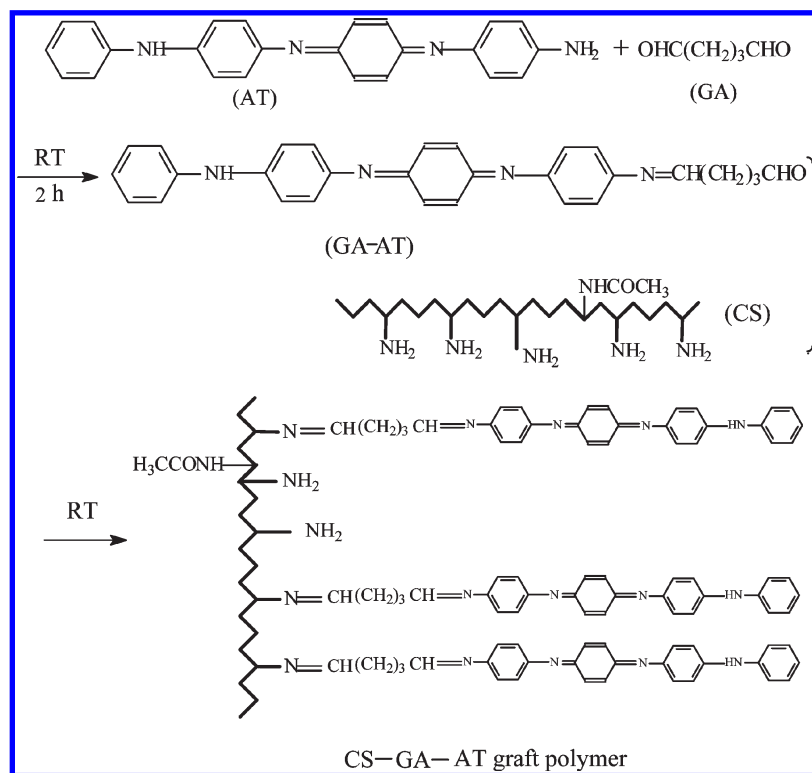
polyaniline (PAN), polypyrrole, and polythiophene, with their special optical and electrical properties, find wide applications in the biomedical area.<sup>24–27</sup> PAN is one of the most extensively studied conducting polymers because of its excellent combination of properties, stability, and easy synthesis.<sup>28,29</sup> However, because of its poor solubility in organic solvent and its infusibility, PAN cannot be easily fabricated as a thin film with good mechanical properties, and PAN is not degradable, which limits its applications. Aniline oligomers with a well-defined structure, good solubility in common solvents, good biocompatibility, and excellent electroactivity similar to that of PAN are attracting great attention.<sup>30–33</sup> We anticipate that by adding aniline oligomer conductive segment to polysaccharides we would obtain degradable and conductive polysaccharide hydrogels that combine the good film-forming properties, biocompatibility, and biodegradability of polysaccharides and the electroactivity of aniline oligomers. By using aniline oligomer, we also overcome the nondegradability of CS-graft-PAN copolymers and hydrogels,<sup>34</sup> whereby the degradation of CS leaves the nondegradable PAN in the body. The AT segments from the degradation of the hydrogels would be consumed by macrophages, reducing the long-term adverse response.<sup>35</sup> Our goal was to develop a simple method for synthesizing degradable and conductive hydrogels. We hypothesize that CS with a large number of amino groups could be functionalized by conductive AT and cross-linked by GA in a one-pot reaction.

**Received:** March 21, 2011

**Revised:** May 13, 2011

**Published:** May 16, 2011

Scheme 1. Synthesis Path of GA-AT and CS-GA-AT Graft Polymer



GA was used to cross-link CS to the AT segment. This avoids the multistep reactions that were used for the synthesis of degradable and conductive hydrogels based on polyesters in our previous paper.<sup>36,37</sup> The formation process, electrical conductivity, surface morphology, and swelling behavior of the hydrogels were investigated.

## EXPERIMENTAL PART

**Materials.** CS (molecular weight 150 000) was obtained from Aldrich, with a degree of deacetylation shown by FT-IR to be 80%.<sup>38</sup> GA (50 wt % in  $\text{H}_2\text{O}$ ) was diluted to a 5 wt % aqueous solution. *N*-Phenyl-1,4-phenylenediamine, ammonium persulfate ( $(\text{NH}_4)_2\text{S}_2\text{O}_8$ ), ammonium hydroxide ( $\text{NH}_4\text{OH}$ ), hydrochloric acid (HCl), acetic acid, dimethylformamide (DMF), and tetrahydrofuran (THF) were all purchased from Aldrich and were used as received.

**Synthesis of Aniline Tetramer.** The synthesis of aniline tetramer (AT) was carried out by following the procedure reported in ref 39. In brief, 4-aminodiphenylamine (18.525 g, 0.10 mol) was dissolved in a mixture of acetone and 1 mol/L HCl (V/V 150:100) at 0 °C in an ice bath. Ammonium persulfate (0.2 mol) in acetone/HCl solution was then added drop by drop to the above solution during 30 min with vigorous stirring. The reaction was carried out in air for 2 h. The mixture was filtered to collect the AT, and the cake was then washed with 30 mL of 1 mol/L HCl and 80 mL of distilled water. The AT was dedoped in 1 mol/L  $\text{NH}_4\text{OH}$  for 2 h and was filtered and washed until the filtrate was neutral. Finally, the AT was dried in a vacuum oven for 72 h. The  $^1\text{H}$  NMR spectrum of AT is shown in Figure 2a.  $^1\text{H}$  NMR (400 MHz,  $\text{DMSO}-d_6$ ): 8.36 (s, 1H), 7.23 (t, 2H), 7.07 (s, 4H), 7.04–6.96 (m, 5H), 6.91–6.82 (m, 2H), 6.83–6.79 (m, 2H), 6.62–6.60 (m, 2H), 5.54 (s, 2H). These results are consistent with data in the literature.<sup>40</sup>

**Table 1. Feed Compositions of the Hydrogels with Different AT Contents and Degree of Crosslinking**

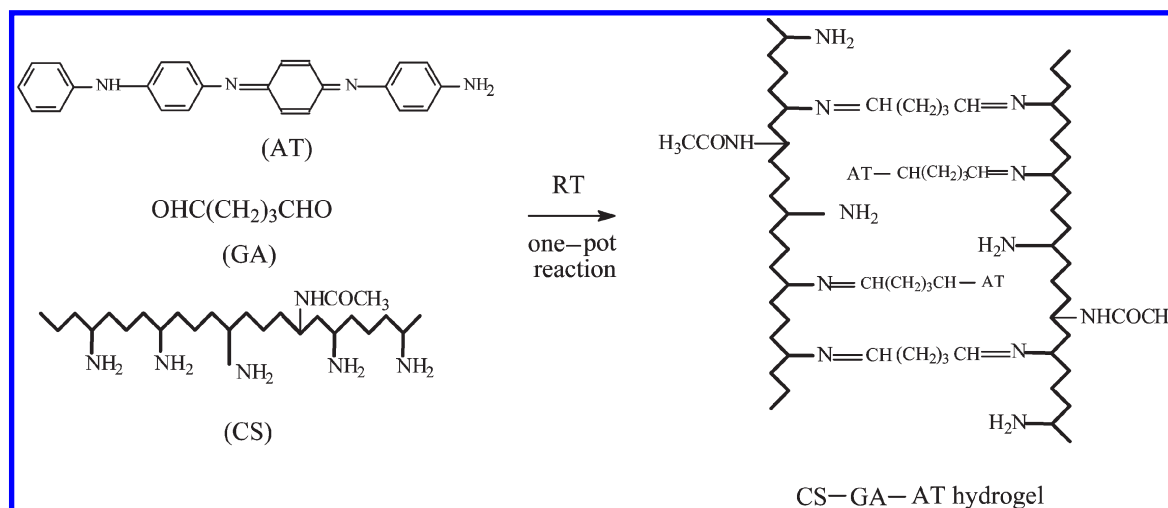
sample code	CS (mg)	AT (mg)	5 wt % GA solution (mg)	2 wt % acetic acid (mL)	DMF (mL)
A1	50	0	87	4	1
A2	50	6	120	4	1
A3	50	9	136	4	1
A4	50	14	161	4	1
A5	50	20	196	4	1
A6	50	26	228	4	1
B1	50	14	120	4	1
B2	50	14	200	4	1
B3	50	14	240	4	1

**Synthesis of GA-AT.** We dissolved 0.187 g AT in 4 mL of DMF, and 0.102 g 50 wt % GA solution was added to the solution. The reaction was conducted at room temperature for 2 h. The mixture was precipitated in 100 mL of cold ether. The product was dried in a vacuum oven at room temperature for 48 h. The synthesis path is shown in Scheme 1.

**Synthesis of CS-GA-AT Graft Polymer.** CS (0.05 g) was dissolved in 3 mL of 1% acetic acid. After reacting for 2 h, the GA and AT mixture was added to the above solution, and the mixture was then vigorously stirred for 10 min. The reaction was kept for 12 h at room temperature, and the polymer was then precipitated in ethanol and dried in a vacuum oven for 48 h. The synthesis route is also shown in Scheme 1.

**Synthesis of CS-GA-AT Hydrogels.** The hydrogels were synthesized in a one-pot reaction. We mixed together 0.05 g CS, which was dissolved in 3 mL of 1% acetic acid and different amount of AT (Table 1) dissolved in 1 mL of DMF, and an appropriate amount of GA (Table 1)

Scheme 2. Schematic Synthesis of CS-GA-AT Hydrogels in a One-Pot Reaction



in a vial by stirring for 10 min. The reaction was then kept for 24 h at room temperature without stirring. The hydrogel was removed from the vial and was immersed in  $\text{H}_2\text{O}/\text{THF}$  mixture for 2 days to extract the unreacted monomer. Finally, the hydrogel was dried in air. The hydrogel synthesis is shown in Scheme 2. The preparation parameters of all samples are listed in Table 1.

Hydrogels with the same cross-linking density but containing different amounts of AT were synthesized by adding various amounts of AT to the solution, and samples having 0, 10, 15, 20, 25, and 30% mass ratio of AT in the hydrogel were designated as A1, A2, A3, A4, A5, and A6, as shown in Table 1.

Hydrogels with different cross-linking densities were prepared by the addition of different amounts of GA solution and are coded as B1, B2, and B3 in Table 1.

The films of the hydrogels named A1, A2, A3, A4, A5, and A6 were prepared by a solution casting method. The mixtures of the solution with the same composition of A1–A6 after stirring for 10 min were cast in Petri dishes, and the solvent was allowed to evaporate in the air for 3 days. The hydrogel films were obtained by removing the films from the Petri dish, and the films were then purified using the same methods as those for the hydrogels. These films were later used for the conductivity tests.

**Characterization.** FT-IR spectra of AT, GA-AT, CS, CS-GA-AT graft polymers and CS-GA-AT hydrogels were obtained using a “Perkin Elmer Spectrum 2000” spectrometer (Perkin-Elmer Instrument, Inc.). Each spectrum was recorded as the average of 16 scans at a resolution of  $4\text{ cm}^{-1}$  in the range between 4000 and  $600\text{ cm}^{-1}$ .

$^1\text{H}$  NMR (400 MHz) spectra of AT, GA-AT, and CS-GA-AT graft polymer were obtained on a Bruker Avance 400 MHz NMR instrument with  $\text{DMSO}-d_6$  as solvent at room temperature and internal standard ( $\delta\ 2.50$ ). In the case of the CS-GA-AT graft polymer, one drop of  $\text{D}_2\text{O}$  was added to the  $\text{DMSO}-d_6$  solution.

The UV–vis spectra of AT, GA-AT, and CS-GA-AT graft polymers were recorded with a UV–vis spectrophotometer (UV-2401) using DMSO as solvent.

We determined the swelling ratio (SR) of the hydrogels by immersing the dry hydrogels in aqueous solutions of the desired pH in sealed vials. The hydrogels were withdrawn from the solution after regular periods of time and weighed after the removal of excess surface water with a filter paper and were then returned to the same vial until swelling equilibrium was established. SR was calculated from the equation:  $\text{SR} = (W_s - W_d) / W_d \times 100\%$ , where  $W_s$  and  $W_d$  are the weights of the swollen and dry-state samples, respectively.

Thermogravimetric analysis (TGA) of the hydrogel samples was used to determine the thermal stability of the hydrogels. TGA tests were conducted under a nitrogen atmosphere (nitrogen flow rate  $50\text{ mL}/\text{min}$ ) with a heating rate of  $10\text{ }^\circ\text{C}/\text{min}$  from 50 to  $800\text{ }^\circ\text{C}$ .

The morphology of the hydrogels before and after swelling mounted on metal stubs was examined using a table-top scanning electron microscope (TM-1000, Hitachi, Japan). The hydrogel samples after swelling were freeze-dried with a freeze-dryer (Heto, Lyolab 3000).

The electrical conductivity of the  $1\text{ mol/L}$  HCl-doped hydrogel films was determined by the standard Van Der Pauw four-probe method.<sup>34,36</sup> The films after doping were thoroughly dried in a vacuum oven for 48 h. The conductivity of the hydrogel film is thus not affected by the water content in the film. The films were cut into a  $1 \times 1\text{ cm}$  square with a thickness between 0.035 and  $0.050\text{ cm}$ . The conductivity of each sample was determined three times at different current values, and the average value was taken as the conductivity of the material.

## RESULTS AND DISCUSSION

**Synthesis of CS-GA-AT Hydrogels.** A facile synthesis of degradable and conductive hydrogels was proposed in this Article. The reactions were based on the aldehyde groups of GA and amino groups of AT and CS. GA is a common cross-linking agent for CS, and GA-cross-linked CS hydrogels are widely used in the biomedical field.<sup>18,41</sup> GA was used as cross-linking agent for CS in this Article. Because GA has two aldehyde groups, we suggest that one aldehyde group would react with the amino group of AT and that the other aldehyde group would react with an amino group on the CS main chain. The electroactive and conductive AT segments would thus be chemically connected to the CS main chain. GA was therefore used as coupling agent for the AT segment and cross-linking agent for the CS at the same time. As a result, CS-GA-AT hydrogels were synthesized in a one-pot reaction with a mixture of CS, GA, and AT at room temperature.

FT-IR and  $^1\text{H}$  NMR spectra were used to characterize the hydrogel. First, we verified that the reaction between the aldehyde group of GA and the amino group of AT could take place under room temperature. The FT-IR spectra of AT and GA-AT obtained by the reaction of GA and AT (molar ratio 1:1) after 2 h at room temperature are shown in Figure 1 as curves a and b. In curve a, the two peaks at  $1597$  and  $1495\text{ cm}^{-1}$  are assigned to the vibration

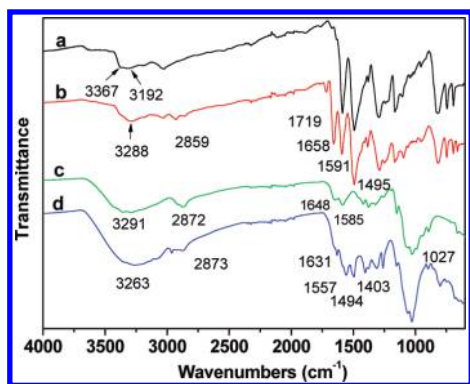


**Figure 1.** FT-IR spectra of (a) AT, (b) GA-AT, (c) CS, and (d) CS-GA-AT graft polymer.

of the quinoid ring and benzene ring in AT. The characteristic absorbance peaks at 3367 and 3192  $\text{cm}^{-1}$  correspond to the amine  $-\text{NH}_2$  group. However, these two peaks changed into a single peak at 3288  $\text{cm}^{-1}$  in curve b of GA-AT because of the disappearance of amine group in AT, which demonstrated that a reaction has occurred between the amino group of AT and the aldehyde group of GA. In addition, a new peak at 1658  $\text{cm}^{-1}$  corresponding to the Schiff base group ( $-\text{N}=\text{CH}-$ ) appeared in curve b of GA-AT, which further indicated that a reaction between the amino group and aldehyde group was taking place.<sup>42</sup> The peak at 1719  $\text{cm}^{-1}$  is the characteristic absorption of the aldehyde group of GA, which means that the aldehyde groups did not react with the secondary amine group in AT. The peak at 2859  $\text{cm}^{-1}$  is from the  $-\text{CH}_2-$  groups of GA. In the next step, we demonstrated that the GA-AT could react with CS solution at room temperature. The FT-IR spectra of CS (c) and CS-GA-AT graft polymer (d) are also shown in Figure 1. Curve c of nonmodified CS shows signals at 1648 and 1585  $\text{cm}^{-1}$  for  $-\text{CO}-$  stretching (amide) and  $\text{N}-\text{H}$  bending (amine), respectively. When the GA-AT reacted with CS, the peak at 1719  $\text{cm}^{-1}$  disappeared, and a new peak appeared at 1631  $\text{cm}^{-1}$  corresponding to the formation of the  $-\text{CH}=\text{N}-$  groups by a coupling reaction between amino groups of CS with aldehyde groups of GA, which demonstrated that the reaction between CS and GA had occurred.<sup>43</sup> Curve d for the CS-GA-AT graft polymer has all of the characteristic peaks of curves b and c, and the peak corresponding to  $-\text{OH}$  and  $-\text{NH}_2$  groups at  $\sim 3263$   $\text{cm}^{-1}$  is broader and shifted to lower wavenumbers than in the curve c of CS, where it appeared at 3291  $\text{cm}^{-1}$ . This indicates that strong hydrogen bonds are formed between the CS and AT. The FT-IR spectra of the CS-GA-AT graft polymer and the CS-GA-AT hydrogels have similar absorptions.

The reaction process was confirmed by the NMR spectrum. The  $^1\text{H}$  NMR spectra of (a) AT, (b) GA, (c) GA-AT, and (d) CS-GA-AT graft polymer are shown in Figure 2. The peak at 9.7 ppm in Figure 2b corresponds to the aldehyde groups in GA. The signals for the  $-\text{NH}_2$  and  $-\text{NH}-$  groups in AT (Figure 2a) are present at 5.5 and 8.3 ppm, respectively. However, the peak at 5.5 ppm has totally disappeared in Figure 2c for GA-AT, indicating that a reaction has occurred between the  $-\text{NH}_2$  group in AT and the aldehyde group in GA, even though the reaction was carried out in room temperature for 2 h. The aldehyde peak at 9.7 ppm and the secondary amine group ( $-\text{NH}-$ ) peak at 8.3 ppm are still present in Figure 2c after the reaction of GA with AT, which suggests that there is no reaction between the

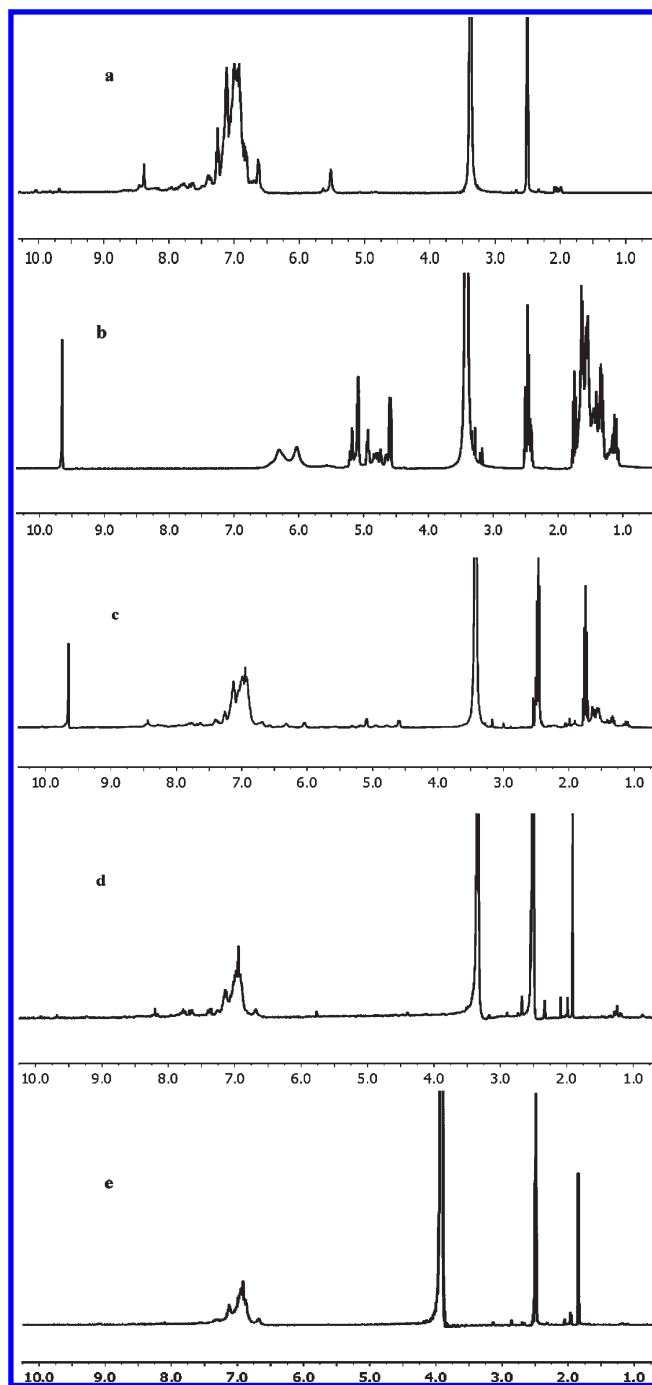


**Figure 2.**  $^1\text{H}$  NMR spectra of (a) AT, (b) GA, (c) GA-AT, (d) CS-GA-AT graft polymer, and (e) CS-GA-AT graft polymer with one drop of  $\text{D}_2\text{O}$  in  $\text{DMSO}-d_6$ .

secondary amine group ( $-\text{NH}-$ ) of AT and aldehyde groups of GA. This offers the opportunity to continue the reaction with CS and will also keep the integral structure of AT segments in the hydrogels. Compared with Figure 2c, the peak of the aldehyde group is absent in Figure 2d because of the reaction between the aldehyde group of GA-AT and the amino group of CS. At the same time, small peaks appear at 1.9, 2.0, and 2.1 ppm, which are ascribed to the different protons of  $-\text{CH}_2-$  groups in the CS chain. When one drop of  $\text{D}_2\text{O}$  was added to the solution of CS-GA-AT, the wide absorption peak at 3.3 ppm in Figure 2d shifted



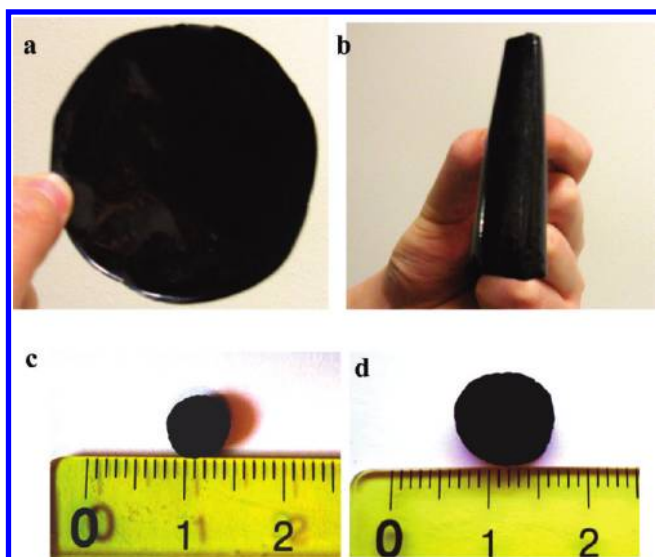
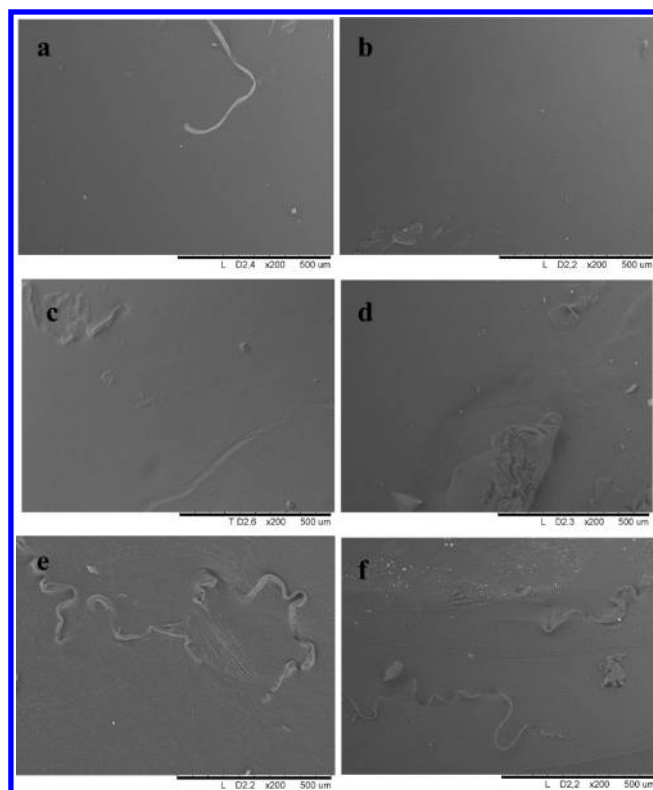


**Figure 3.** (a) Free-standing, (b) flexible degradable, and electrically conductive hydrogel films (sample A4) from CS, GA, and AT solutions in a one-pot reaction, (c) A4 hydrogel in the dry state, and (d) A4 hydrogel after swelling in a pH 2.1 solution for 48 h.

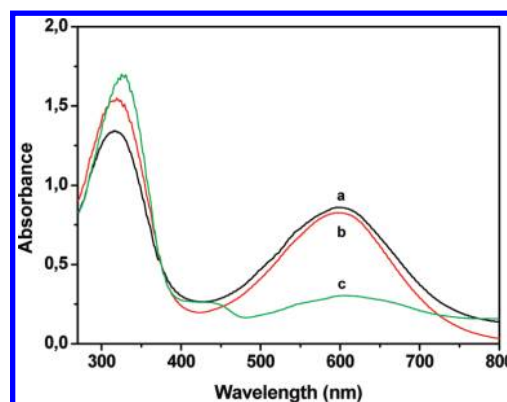
to 3.9 ppm in Figure 2e, which is ascribed to the specific peak of hydroxyl groups in the CS that overlapped the signal for the H<sub>2</sub>O protons.<sup>44</sup> It was also found that the secondary amine groups (–NH–) in the AT segment in the CS-GA-AT graft polymer completely disappeared in Figure 2e because of the proton exchange with D<sub>2</sub>O. This also indicated that the –NH– groups are still present in AT.<sup>34</sup> The integrality of the AT structure was thus kept, and the electroactivity and conductivity of AT remained.

Photographs of the hydrogel films and hydrogels obtained are shown in Figure 3. Figure 3a,b shows the free-standing, flexible degradable and conductive hydrogel films (sample A4). This overcomes the drawback with PAN, which could not be easily fabricated into thin films in common organic solvents. Figure 3c, d shows the hydrogel before and after swelling in pH 2.1 buffer solutions. It is obvious that the hydrogel has a much larger volume after swelling than in the dry state. The morphologies of the hydrogels investigated were characterized by SEM, and the results are shown in Figure 4. All hydrogels have a condensed surface, and the surfaces become rougher with increasing AT content in the hydrogels. This phenomenon is similar to that of CS-graft-PAN membranes.<sup>45</sup>

The electroactivity was confirmed by the UV spectra of (a) AT, (b) GA-AT, and (c) CS-GA-AT graft polymers shown in Figure 5. Curve a for AT in the emeraldine state shows two absorption peaks at 320 and 600 nm, which are assigned to the  $\pi$ – $\pi^*$  transition of the benzene ring and to the benzenoid (B) to quinoid (Q)  $\pi_B$ – $\pi_Q$  excitonic transition.<sup>46</sup> Similarly, both the GA-AT and the CS-GA-AT graft polymers exhibit two absorption peaks at 320 and 600 nm, which indicates that the AT segment in the GA-AT and CS-GA-AT graft polymers retains its electroactivity. The Q/B intensity ratio of the GA-AT and CS-GA-AT graft polymers was much lower than that of AT. This can probably be explained by the fact that the –N=CH– group is an electron-withdrawing group compared with the amino –NH<sub>2</sub> group, which reduced the electronic concentration of the quinone units. This also confirmed that a coupling reaction between the amino group and the aldehyde group had occurred.



**Figure 4.** SEM images of the dry hydrogels with different AT contents before swelling: (a) A1, (b) A2, (c) A3, (d) A4, (e) A5, and (f) A6.

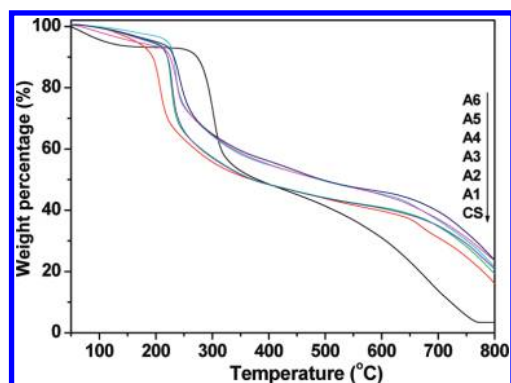


**Figure 5.** UV spectra of (a) AT, (b) GA-AT, and (c) CS-GA-AT graft polymer in DMSO solution.

**Conductivity of the Hydrogels.** The electrical conductivities of the hydrogel films with different AT contents after doping with the 1 mol/L HCl were determined by a standard four probe technique, and the conductivity data are listed in Table 2. The conductivity of the pure CS film was  $\sim 3.13 \times 10^{-8}$  S/cm, because of the ionic conductivity of the ionized –NH<sub>3</sub><sup>+</sup> group in the hydrogels.<sup>47</sup> When 10% AT was grafted to the hydrogel, the conductivity increased to  $2.97 \times 10^{-7}$  S/cm, which is  $\sim 9.5$  times higher than that of a pure CS hydrogel film. The conductivity of the hydrogels is a combination of ionic conductivity from CS and electrical conductivity from AT. However, it is clear that the main contribution to the conductivity of the hydrogel is from AT segment. The conductivity of the hydrogel increased from

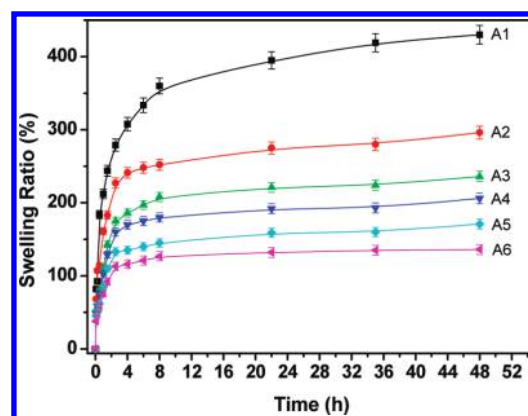
**Table 2.** Conductivity and Weight Loss of CS-GA-AT Hydrogels with Different AT Content

sample name	conductivity (S/cm)	AT content	weight loss (pH 2.1)	weight loss (pH 7.4)
A1	$3.13 \times 10^{-8}$	0%	7.8%	6.2%
A2	$2.97 \times 10^{-7}$	10%	11.7%	10.6%
A3	$6.84 \times 10^{-7}$	15%	12.4%	10.5%
A4	$2.11 \times 10^{-6}$	20%	13.9%	12.5%
A5	$7.65 \times 10^{-6}$	25%	12.7%	13.8%
A6	$2.94 \times 10^{-5}$	30%	12.1%	12.9%

**Figure 6.** TGA thermograms of hydrogels.

$2.97 \times 10^{-7}$  to  $2.94 \times 10^{-5}$  S/cm when the AT content was increased from 10 to 30% in the hydrogels. This can be explained by the fact that the AT segments in the network have a greater chance to form interconnected conductive network structures when the AT content is higher in the polymer matrix. The strong hydrogen bonds between the hydrogen donor  $-\text{NH}-$  group of AT and hydrogen acceptor amide group along the CS backbone may also help the electron transfer between the AT segments.<sup>34,48</sup> The broad range of electrical conductivities of these hydrogel films provides a wide choice for specific biomedical applications. The conductivity of these hydrogel films is lower than that of the reference CS-graft-PAN hydrogels, which is  $\sim 10^{-2}$  S/cm when the PAN content is 45 wt %.<sup>34</sup> This is because the conductivity of the AT segment is much lower than that of PAN. However, the conductivity of these hydrogel films is sufficient for electrical stimulation on the cell proliferation and differentiation<sup>33</sup> because the microcurrent *in vivo* is quite low.

**Thermal Properties of the Hydrogels.** The TGA thermograms of pristine CS and samples A1, A2, A3, A4, A5, and A6 are plotted in Figure 6. The CS shows an obvious weight loss between 50 and 160 °C, which is attributed to a loss of water. However, there is a small weight loss for samples A1 to A6 because the GA-cross-linked CS hydrogel and the hydrogels with different AT contents are much more hydrophobic than CS because of the cross-linking reaction of GA<sup>49</sup> and the more hydrophobic nature of the AT segment. Samples A1–A6 have a lower thermal stability than pure CS, below 410 °C for samples A1–A3 and below 320 °C for samples A4–A6, which is probably because the introduction of a rigid AT segment into the hydrogel interrupts the crystallization of the CS. This leads to a decrease in the crystallinity of the hydrogel. The thermal stability of the cross-linked hydrogels is higher than that of CS, from 320 to 410 °C depending on the AT content, because the cross-linking

**Figure 7.** Swelling ratio as a function of time for CS-GA-AT hydrogels with different AT contents in pH 2.1 solution.

between the CS chains restricts the movement of the chains. There is a smaller weight loss at 800 °C with a higher AT content because the conjugated AT segments have much greater thermal stability than CS.

**Swelling Behavior of the Hydrogels.** The SR of these hydrogels is dependent on the AT content, the pH of the solution, and the degree of cross-linking of the hydrogel. By changing these parameters, we can tune the SR of these hydrogels to meet any specific biomedical application.

The effect of AT content on the SR of the hydrogels is shown in Figure 7. Sample A1 swells most rapidly, and it has the highest SR among these samples. The SRs of the samples decreased with increasing AT content in the hydrogel. The  $\text{pK}_a$  of CS is 6.2 to 7.0, which means that the  $-\text{NH}_2$  groups along the CS chain will be positively charged because of protonation in the pH 2.1 solution.<sup>50</sup> The hydrogen bonds between the  $-\text{NH}_2$  group,  $-\text{OH}$  group, and amide group will break, and the electrostatic repulsions between the  $-\text{NH}_3^+$  groups will make the hydrogel network expand.<sup>51</sup> The SR of sample A1 therefore increased most rapidly. With a higher AT content in the hydrogels, more  $-\text{NH}_2$  groups in the CS are consumed by the reaction with GA and AT. The number of  $-\text{NH}_2$  groups in the network will therefore decrease with increasing AT content. The number of hydrogen bonds among the  $-\text{NH}_2$  group,  $-\text{CO}-\text{NH}-$  amide group, and  $-\text{OH}$  group increased, as indicated by the FT-IR spectra (Figure 1d). As a result, the driving force for expansion decreased, and the driving force for contraction increased with increasing AT content in the sample. The SR thus decreased with increasing AT content. The hydrogels with different AT contents were freeze-dried after swelling, and the surface morphology was observed by SEM, as shown in Figure 8. The surfaces of the hydrogels were much rougher than before swelling (Figure 4). The holes and cracks in the hydrogels (Figure 8) serve as channels that allow water molecules to diffuse inside the hydrogels. In the case of the CS sample, the surface before swelling was quite smooth, as shown in Figure 4a, and there were many small holes after swelling, as shown in Figure 8a. The size and numbers of holes and cracks on the surface decreased with increasing AT content in the hydrogel, as shown in Figure 8b–f.

The effect of the pH of the solution on the SR of sampled A1–A6 is shown in Figure 9. The SRs of the hydrogels are much higher in pH 2.1 solution than in pH 7.4 solution. This is because the  $-\text{NH}_3^+$  groups in the network that cause the electrostatic repulsion in the hydrogel network in pH 2.1 solution are transformed

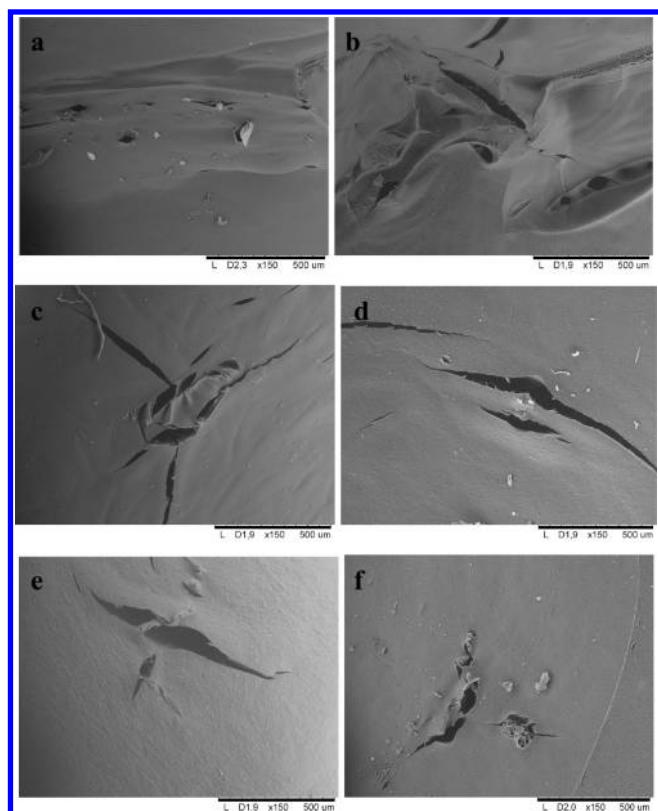


**Figure 8.** SEM images of CS-GA-AT hydrogels with different AT contents after swelling for 48 h in pH 2.1 solution and subsequent after freeze-drying: (a) A1, (b) A2, (c) A3, (d) A4, (e) A5, and (f) A6.

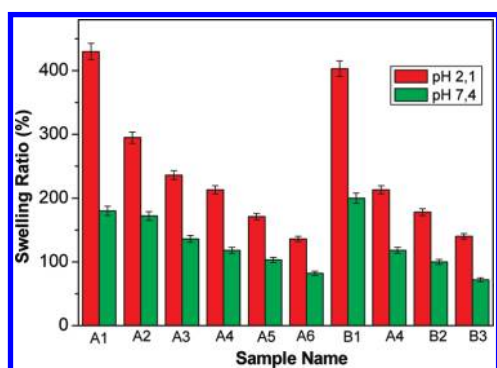


**Figure 9.** Effect of pH and cross-linking agent content on the swelling ratio of the hydrogels.

into  $-\text{NH}_2$  groups in the pH 7.4 buffer solution. The H-bonds between the  $-\text{NH}_2$ ,  $-\text{OH}$ ,  $-\text{NH}-$ , and  $-\text{CO}-\text{NH}-$  groups increased because of the increasing number of  $-\text{NH}_2$  groups in pH 7.4 solution. These two reasons lead to a decrease in the SR of the hydrogels in pH 7.4 solution. This was confirmed by the FT-IR spectra of hydrogels dried from the pH 2.1 solution (Figure 10a) and from the pH 7.4 solution (Figure 10b). In Figure 10a, the peak at  $1595\text{ cm}^{-1}$  assigned to the absorption of the quinoid ring was absent, and a new peak at  $1557\text{ cm}^{-1}$  appeared, probably because of the protonation of  $-\text{NH}-$  groups connected to the quinoid ring and the symmetric deformation of the  $-\text{NH}_3^+$  group resulting from ionization of primary amino groups in the acidic medium (pH 2.1).<sup>52</sup> The characteristic absorption of  $-\text{NH}_2$

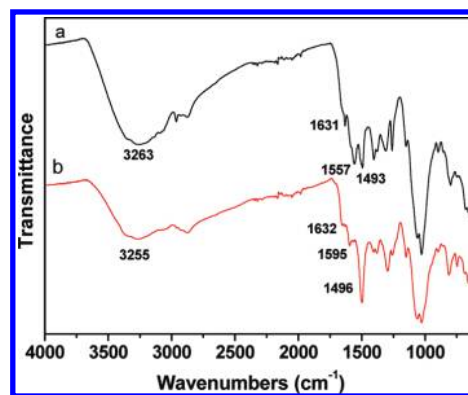


**Figure 10.** FT-IR spectra of hydrogels from (a) pH 2.1 solution and (b) pH 7.4 solution.

and  $-\text{OH}$  groups at  $3263\text{ cm}^{-1}$  in Figure 10a shifted to lower wavenumbers at  $3255\text{ cm}^{-1}$  and was broader than that in curve b (Figure 10), indicating that the number of hydrogen bonds between  $-\text{NH}_2$ ,  $-\text{OH}$ ,  $-\text{NH}-$ , and  $-\text{CO}-\text{NH}-$  groups was greater in the hydrogel network from pH 7.4 buffer solution.

The degree of cross-linking of the hydrogels also had a great effect on the SR of the hydrogels. By adding different amounts of GA to the mixture, a series of hydrogels B1–B3 were obtained with different SRs, and the effect of pH and GA content on the SR of these hydrogels is also shown in Figure 9. It was found that the SR of these hydrogels decreased with increasing GA content. More  $-\text{NH}_2$  groups were consumed by the GA with increasing GA content, and the hydrophilicity of the hydrogel decreased. The surface morphologies after swelling of the hydrogels with different GA contents are shown in Figure 11. Many intersections can be seen between the deep and long channels of sample B1, and the size and numbers of these cracks decreases dramatically with increasing amount of cross-linker. The surface of sample B3 is quite smooth. The surface morphology thus provides a reasonable explanation of the swelling behavior of these hydrogels with different degrees of cross-linking. Figure 9 also shows that the SR of samples having a given amount of GA is greater in the acidic solution than in pH 7.4 solution. We thus obtained a series of hydrogels with tunable SRs by changing the AT content, the pH value of the solution, and the GA content in the samples. The SRs of these hydrogels are somewhat higher than that those in our previous papers,<sup>36,37</sup> and this means that they have a wider range of applications.

**Degradation of the Hydrogels.** GA was used as cross-linker to generate a CS network and as coupling agent for AT to graft it to the side groups of the CS chain, as shown in Scheme 2. Our motive for using AT was that it may be consumed by macrophages and subsequently undergo renal clearance, thereby avoiding an adverse response.<sup>35</sup> Consequently, the whole CS network bearing ATs as side chains is degradable. To study the degradation of the hydrogels, we dried the samples after they had been immersed in the pH 2.1 and 7.4 buffer solutions for 48 h and then weighed them. The weight loss is defined as  $\text{weight loss} = (W_o - W_i)/W_i \times 100\%$ , where  $W_o$  and  $W_i$  are, respectively, the weight of dry hydrogel after extraction by  $\text{H}_2\text{O}/\text{THF}$  solution and the weight of the vacuum-dried hydrogel after swelling for 48 h. The weight loss data are shown in Table 2. The hydrogels suffered a 6.2–13.9% weight loss during the swelling for 48 h, indicating that these hydrogels can undergo slow degradation in these buffer solutions. This may be ascribed to the degradation of



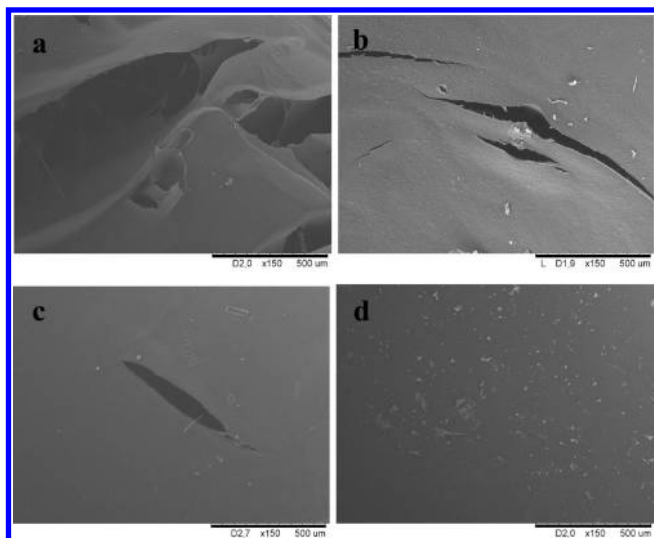


**Figure 11.** SEM images of CS-GA-AT hydrogels with different cross-linking agent contents after swelling for 48 h in pH 2.1 solution: (a) B1, (b) A4, (c) B2, and (d) B3.

the CS main chain and cleavage of the Schiff base group because of its instability. Furthermore, the difference of the weight loss of the GA cross-linked CS hydrogels and the hydrogels with AT segments are relatively small. In addition, the absorption of benzene ring at  $1493\text{ cm}^{-1}$  remained in the FT-IR spectrum of hydrogel after 48 h of swelling in pH 2.1 solution, as shown in Figure 10a. This indicates that a certain portion of AT units are still conjugated to the CS chain after being exposed to low pH.

## CONCLUSIONS

We have demonstrated a facile method of synthesis of degradable and electrically conductive hydrogels (DECHs) based on CS and AT. This avoids the multiple step reactions used for the preparation of DECHs based on polyesters in our previous work. A series of degradable and conductive hydrogels and their free-standing flexible films have been successfully synthesized by a one-pot reaction under mild conditions with a combination of degradability, the good film-forming properties of CS, and the electrical conductivity of aniline oligomer. The electroactivity of the hydrogel is confirmed by FT-IR, NMR, and UV studies. The conductivity of the hydrogels, mainly from AT segments, varied from  $2.94 \times 10^{-5}$  to  $2.97 \times 10^{-7}\text{ S/cm}$  when the AT content decreased from 30 to 10%. The SR of the hydrogel is dependent on the AT content, the GA content, and the pH values. The swelling behavior is verified by FT-IR and SEM. Because of the commercial availability of CS, this facile synthesis method leads to new possibilities for the large-scale preparation of degradable and conductive hydrogels and their films.

## AUTHOR INFORMATION

### Corresponding Author

\*Tel: +46-8-790 8274. Fax: +46-8-20 84 77. E-mail: aila@polymer.kth.se.

## ACKNOWLEDGMENT

We are grateful to the Swedish Research Council (grant no. 2008-5538), the China Scholarship Council (CSC), and The

Royal Institute of Technology (KTH) for financial support for this work.

## REFERENCES

- (1) Peppas, N. A.; Hilt, J. Z.; Khademhosseini, A.; Langer, R. *Adv. Mater.* **2006**, *18*, 1345–1360.
- (2) Coviello, T.; Matricardi, P.; Marianecci, C.; Alhaique, F. *J. Controlled Release* **2007**, *119*, 5–24.
- (3) Roos, A. A.; Edlund, U.; Sjöberg, J.; Albertsson, A. C.; Stalbrand, H. *Biomacromolecules* **2008**, *9*, 2104–2110.
- (4) Albertsson, A. C.; Voepel, J.; Edlund, U.; Dahlman, O.; Soderqvist-Lindblad, M. *Biomacromolecules* **2010**, *11*, 1406–1411.
- (5) Edlund, U.; Albertsson, A. C. *J. Bioact. Compat. Polym.* **2008**, *23*, 171–186.
- (6) Voepel, J.; Edlund, U.; Albertsson, A. C. *J. Polym. Sci., Part A: Polym. Chem.* **2009**, *47*, 3595–3606.
- (7) Voepel, J.; Edlund, U.; Albertsson, A. C.; Percec, V. *Biomacromolecules* **2011**, *12*, 253–259.
- (8) Voepel, J.; Edlund, U.; Albertsson, A. C. *J. Polym. Sci., Part A: Polym. Chem.* **2011**, *49*, 2366–2372.
- (9) Dutta, P. K.; Ravikumar, M. N.; Dutta, J. J. *Macromol. Sci., Polym. Rev.* **2002**, *C42*, 307–354.
- (10) Guo, B. L.; Yuan, J. F.; Gao, Q. Y. *Colloids Surf., B* **2007**, *58*, 151–156.
- (11) Rinaudo, M. *Prog. Polym. Sci.* **2006**, *31*, 603–632.
- (12) Sashiwa, H.; Aiba, S. I. *Prog. Polym. Sci.* **2004**, *29*, 887–908.
- (13) Guo, B. L.; Yuan, J. F.; Gao, Q. Y. *J. Mater. Sci., Mater. Med.* **2007**, *18*, 753–757.
- (14) Guo, B. L.; Yuan, J. F.; Yao, L.; Gao, Q. Y. *Colloid Polym. Sci.* **2007**, *285*, 665–671.
- (15) Qu, X.; Wirsén, A.; Albertsson, A. C. *Polymer* **2000**, *41*, 4589–4598.
- (16) Qu, X.; Wirsén, A.; Albertsson, A. C. *J. Appl. Polym. Sci.* **1999**, *74*, 3193–3202.
- (17) Qu, X.; Wirsén, A.; Albertsson, A. C. *Polymer* **2000**, *41*, 4841–4847.
- (18) Mi, F. L.; Kuan, C. Y.; Shyu, S. S.; Lee, S. T.; Chang, S. F. *Carbohydr. Polym.* **2000**, *41*, 389–396.
- (19) Crescenzi, V.; Francescangeli, A.; Taglienti, A.; Capitani, D.; Mannina, L. *Biomacromolecules* **2003**, *4*, 1045–1054.
- (20) Wu, X. M.; Black, L.; Santacana-Laffitte, G.; Patrick, C. W. *J. Biomed. Mater. Res., Part A* **2007**, *81A*, 59–65.
- (21) Shi, J.; Alves, N. M.; Mano, J. F. *Macromol. Biosci.* **2006**, *6*, 358–363.
- (22) Guo, B. L.; Gao, Q. Y. *Carbohydr. Res.* **2007**, *342*, 2416–2422.
- (23) Wong, J. Y.; Langer, R.; Ingber, D. E. *Proc. Natl. Acad. Sci. U.S.A.* **1994**, *91*, 3201–3204.
- (24) Guimard, N. K.; Gomez, N.; Schmidt, C. E. *Prog. Polym. Sci.* **2007**, *32*, 876–921.
- (25) MacDiarmid, A. G. *Angew. Chem., Int. Ed.* **2001**, *40*, 2581–2590.
- (26) Heeger, A. J. *Angew. Chem., Int. Ed.* **2001**, *40*, 2591–2611.
- (27) Ravichandran, R.; Sundarajan, S.; Venugopal, J. R.; Mukherjee, S.; Ramakrishna, S. *J. R. Soc., Interface* **2010**, *7*, S559–S579.
- (28) Kang, E. T.; Neoh, K. G.; Tan, K. L. *Prog. Polym. Sci.* **1998**, *23*, 277–324.
- (29) Bhadra, S.; Khastgir, D.; Singha, N. K.; Lee, J. H. *Prog. Polym. Sci.* **2009**, *34*, 783–810.
- (30) Wei, Z. X.; Faul, C. F. J. *Macromol. Rapid Commun.* **2008**, *29*, 280–292.
- (31) Guo, B. L.; Finne-Wistrand, A.; Albertsson, A. C. *Macromolecules* **2010**, *43*, 4472–4480.
- (32) Guo, B. L.; Finne-Wistrand, A.; Albertsson, A. C. *Biomacromolecules* **2010**, *11*, 855–863.
- (33) Huang, L. H.; Zhuang, X. L.; Hu, J.; Lang, L.; Zhang, P. B.; Wang, Y. S.; Chen, X. S.; Wei, Y.; Jing, X. B. *Biomacromolecules* **2008**, *9*, 850–858.

- (34) Marcasuzaa, P.; Reynaud, S.; Ehrenfeld, F.; Khoukh, A.; Desbrieres, J. *Biomacromolecules* **2010**, *11*, 1684–1691.
- (35) Rivers, T. J.; Hudson, T. W.; Schmidt, C. E. *Adv. Funct. Mater.* **2002**, *12*, 33–37.
- (36) Guo, B. L.; Finne-Wistrand, A.; Albertsson, A. C. *Chem. Mater.* **2011**, *23*, 1254–1262.
- (37) Guo, B. L.; Finne-Wistrand, A.; Albertsson, A. C. *J. Polym. Sci., Part A: Polym. Chem.* **2011**, *49*, 2097–2105.
- (38) Brugnerotto, J.; Lizardi, J.; Goycoolea, F. M.; Arguelles-Monal, W.; Desbrieres, J.; Rinaudo, M. *Polymer* **2001**, *42*, 3569–3580.
- (39) Sun, Z. C.; Kuang, L.; Jing, X. B.; Wang, X. H.; Li, J.; Wang, F. S. *Chem. Res. Chin. Univ.* **2002**, *23*, 496–499.
- (40) Rozalska, I.; Kulyk, P.; Kulszewicz-Bajer, I. *New J. Chem.* **2004**, *28*, 1235–1243.
- (41) Yamada, K.; Chen, T. H.; Kumar, G.; Vesnovsky, O.; Topoleski, L. D. T.; Payne, G. F. *Biomacromolecules* **2000**, *1*, 252–258.
- (42) Dufour, B.; Rannou, P.; Travers, J. P.; Pron, A.; Zagorska, M.; Korc, G.; Kulszewicz-Bajer, I.; Quillard, S.; Lefrant, S. *Macromolecules* **2002**, *35*, 6112–6120.
- (43) Guo, B. L.; Yuan, J. F.; Gao, Q. Y. *e-Polym.* **2006**, 082.
- (44) Hosseini, S. H.; Simiari, J.; Farhadpour, B. *Iran. Polym. J.* **2009**, *18*, 3–13.
- (45) Varghese, J. G.; Kittur, A. A.; Rachipudi, P. S.; Kariduraganavar, M. Y. *J. Membr. Sci.* **2010**, *364*, 111–121.
- (46) Wang, H. F.; Guo, P.; Han, Y. C. *Macromol. Rapid Commun.* **2006**, *27*, 63–68.
- (47) Thanpicha, T.; Sirivat, A.; Jamieson, A. M.; Rujiravanit, R. *Carbohydr. Polym.* **2006**, *64*, 560–568.
- (48) Barthet, C.; Armes, S. P.; Chehimi, M. M.; Bilem, C.; Omastova, M. *Langmuir* **1998**, *14*, 5032–5038.
- (49) Beppu, M. M.; Vieira, R. S.; Aimoli, C. G.; Santana, C. C. *J. Membr. Sci.* **2007**, *301*, 126–130.
- (50) Chuah, A. M.; Kuroiwa, T.; Kobayashi, I.; Nakajima, M. *Food Hydrocolloids* **2009**, *23*, 600–610.
- (51) Guo, B. L.; Yuan, J. F.; Gao, Q. Y. *Colloid Polym. Sci.* **2008**, *286*, 175–181.
- (52) Wang, T.; Turhan, M.; Gunasekaran, S. *Polym. Int.* **2004**, *53*, 911–918.